Characterization of potentially-interstellar, nanoparticles condensed in hydrogen atmosphere. Y. Nakano[1], Y. Kimura[1], and A. Hashimoto[2]; [1] Institute of Low Temperature Science, Hokkaido Univ., Sapporo, Japan, (ynakano@lowtem.hokudai.ac.jp), [2] Suns & Fishermen Society, Sapporo, Japan.

Introduction: Dust forms around dying stars and fills in interstellar space. Most of the dust sublimates by intense star radiations, shock waves, etc. [e.g., 1], but atoms and molecules recondense and replenish dust. Interstellar dust must be a mixture of original, star-driven dust and secondary dust regenerated in interstellar environment.

Size, shape, and composition of interstellar dust are estimated by the observed optical features such as extinction, emission, and linear/circular polarization of star light, combined with models [e.g., 2]. Detailed physical and chemical properties of interstellar dust is still provisional [3], partly because characterization of nanoparticles to compare to interstellar dust is poor.

Nanoparticles can be produced in laboratories for their full characterization. Traditionally, experimental techniques that use simultaneous evaporation and condensation in low-pressure ambient gases have been applied to materials with rather simple compositions, including oxides, silicates, metals, carbon, and metal carbides [e.g., 4].

Here we report a preliminary characterization of nanoparticles condensed from the vapor by laser abrasion of a homogenized charge of Allende meteorite (CV3) in a flow of pure H_2 at 1 atm. Allende contains all elements in solar proportions except for volatiles.

Experiment and analysis: An experimental setup designed for laser evaporation and condensation of silicates in ambient gases are described in our previous paper [5]. We use a 1 atm H_2 gas flow and cw-CO_2 laser with a power of 100 W for 3 seconds. A Cu grid is set beforehand on the upper inner wall of the chamber for collecting upward-drifting condensate particles. A gas flow is continuously evacuated with a vacuum pump (6 L/min) through a feedthrough inserted into the upper part of the chamber. A filter is set at the orifice of the feedthrough to collect floating particles.

We use transmission electron microscopy (JEOL JEM-2100F, instrument operated at 200kV) to characterize morphology, structure, and composition of the collected nanoparticles (NPs) and their aggregates.

Results: We collected 66 aggregates of NPs on the Cu grid in one run and some of them are shown in Figure 1. Lone NPs are rare. The aggregates are classified into four types according to their constituent NPs - amorphous silicate NPs (**S**), core/mantle NPs with iron or hydrogenized-iron core and amorphous silicate mantle (**IS**), amorphous silicon oxycarbide NPs and hydrogenized, amorphous silicon oxycarbide NPs (both **SiOC**), and carbon NPs (**C**) (Table 1).

We identify SiOC type according to the morphology and composition of their aggregates akin to the reported silicon oxycarbides [6]. S and IS types are subdivided into three subtypes (a, b, and c in Table 1) according to their NP shape: spherical, fused, and skeletal. C type is subdivided into three groups according to their NP morphology and crystal structures: fullerene, graphitic sheet, and poly-diamond.

From the electron diffraction study, we identify that core metals of IS type NPs are α-iron, that SiOC type is amorphous, and that C type has two kinds of crystals structure: graphite (fullerene and graphitic sheets) and hexagonal-diamond (poly-diamond).

Contrast of the core of IS NPs in the bright field TEM image varies from NPs to NPs, reflecting a range in core density. We emphasize that all NPs are produced in the 1 atm H_2 gas and assume that the iron cores contain different amounts of hydrogen (indicating the range between iron and hydrogenized-iron).

Size and composition of each NP type are listed in Table 1. We point out that the size decreases in the order of a, b, and c (limb width for c) subtypes for the S and IS type NPs. A boundary between the spherical and the fused subtypes is ~30 nm in NP diameter.

Discussion and conclusions: Our results show that at least four types of NP aggregates are produced in one heating event in pure H_2 from the experimental charge. Under the adopted condition, ~ten wt.% of the original mass evaporated and condensed as NPs. Silicon and Fe evaporate earlier than Mg [5], explaining their high contents in NPs of S and IS types. Al, although trace, is contained in S, IS, and SiOC types, perhaps due to a highly reducing condition.

Occurrence of C type is unexpected because of low concentration of C (0.3 wt.%) in Allende [7], while C is a major element in ISM. The average NP size, ~30 nm, for S and IS types explains the interstellar extinction in UV [8]. The metal-core/silicate-mantle structure and skeletal subtypes may explain the interstellar polarization [9]. High temperature atmospheres of exoplanets may bear such nanoparticles [10].

Our experimental system must consider many factors in future, particularly the effect of ambient pressure and thermal convection to have on physical and chemical properties of NPs and their aggregates.

Acknowledgments: We acknowledge staffs of Inst. of Low Temp. Sci. and Dept. of Planets & Space, Hokkaido Univ. for their technical supports.

References: [1] Jones A.P. (2004) ASP conference Series. Vol. 309. 347-367. [2] Mathis J. S. (1990) An-

nu. Rev. Astron. Astrophys. 28, 37-70. [3] Draine B. T. (2004) APS Conference series, Vol. 309. 691-708. [4] Stephens J. R. and Kothari B. K. (1978) The Moon and the Planets 19, 139-152. [5] Nakano Y. and Hashimoto A. (2020) Prog. Earth Planet Sic. 7, 47. [6] Tavakoli A. H. and Armentrout M. M. (2015) J. Mater. Res. 30, 296-303. [7] Jarosewich E. (1990) Meteoritics 25, 323-337. [8] Kim S-H. et al. (1993) ApJ. 422, 164-175. [9] Andersson et al. (2015) Annu. Rev. Astron. Astrophys. 53, 501-539. [10] Potapov A. and Bouwman J. (2022) Front. Astron. Space Sci. 9:12302.

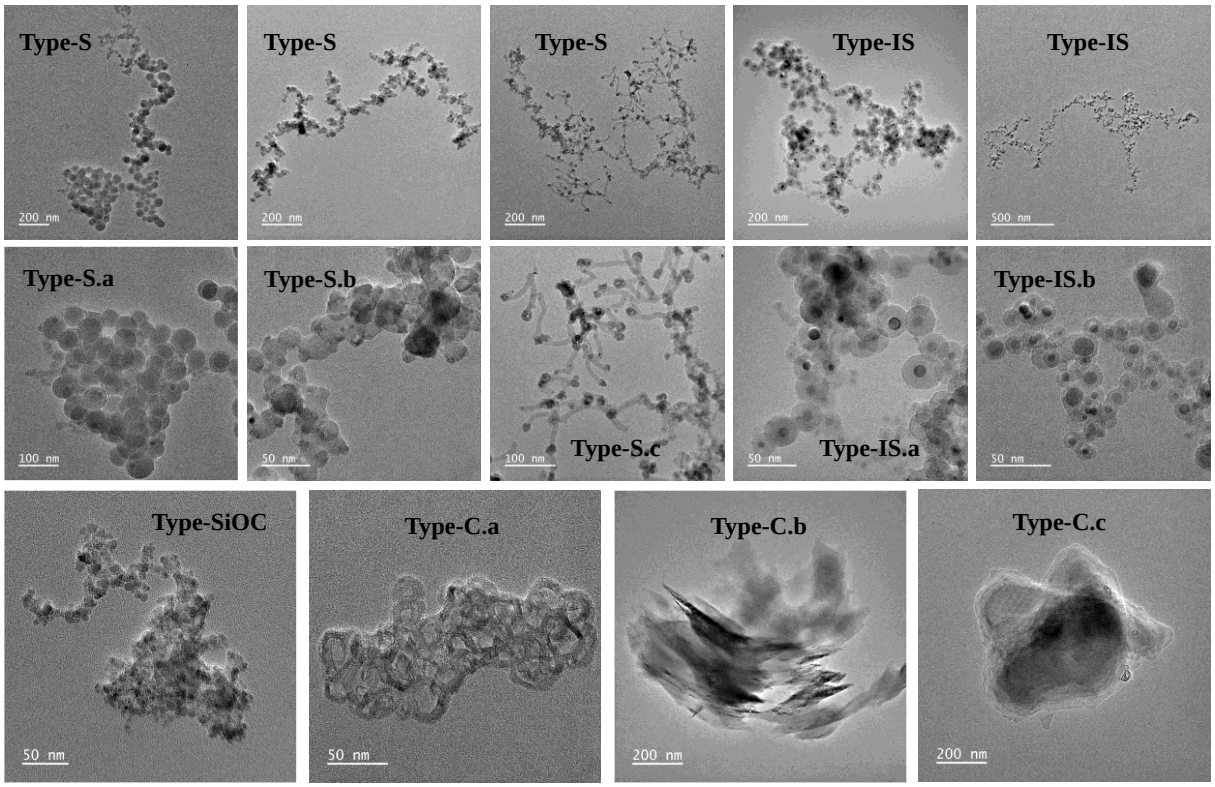

Figure 1. Bright field transmission electron microscope (TEM) images of selected condensed nanoparticle aggregates. Top panels show a whole view of each aggregate. Center panels show blow-ups of the top panels. Bottom panels show type-SiOC and -C.

Table 1. Characterization of the collected condensed nanoparticles

Type	S	IS	SiOC	C
Main component	amorphous silicate	iron, hydrogenized iron, and amorpohus silicate	amorphous silicon oxycarbide and amorphous hydrogenized silicon oxycarbide	carbon
Aggregate morphology	fractal	fractal	massive	compact, massive
NP shape (NP material)	a. spherical (amorp sil) b. fused (amorp sil, with/without cry) c. skeletal (amorp sil limbs, with/without cry ends)	a. spherical (Iron-, hIron-core/amorp sil mantle) b. fused (Iron-, hIron-core/amorp sil mantle with/without cry) c. skeletal (amorp sil limbs with/without Iron-, hIron-joints and cry ends)	granular (amorp silicon oxycarbide, h amorp silicon oxycarbide)	a. onions (fullerene) b. stacked sheets (graphitic sheets) c. lump (poly-diamonds)
Size range of individual NPs	a. 30-70 nm in NP diameter b. 10-30 nm in NP diameter c. 100-120 nm in limb length; 13 nm in limb width	a. 30-50 nm in NP diameter; 10-20 nm in core diameter b. 15-35 nm in NP diameter; 5-15 nm in core diameter c. 70-80 nm in limb length; 10-17 nm in limb width; 5-15 nm core diameter	~20 nm in NP diameter	a. 20-80 nm in fullerene diameter
NP composition	major: O >> Si > Fe trace: Mg, Al, Na	Mantle + Core major: O > Si > Fe >> Mg trace: Al, Na, Cr	major: C ~ O > Si >> Fe, Mg, (Ca) trace: Na, Al, P, S, Cl, K, (N)	major: C trace: O, Si >> Fe
Number of occurrence	17	29	10	10

Abbreviations: sil (silicate); amorp (amorphous); hIron (hydrogenized iron); h (hydrogenized); cry (crystal).